Multifunctional isoxazolidine derivatives as α-amylase and α-glucosidase inhibitors

Ameni Ghabi, Jihed Brahmi, Fahad Alminderej, Sabri Messaoudi, Sébastien Vidal, Adel Kadri, Kaïss Aouadi

Multifunctional isoxazolidine derivatives as α-amylase and α-glucosidase inhibitors

Ameni Ghabi,[a] Jihed Brahmi,[a] Fahad Alminderej,[b] Sabri Messaoudi,[b,c] Sébastien Vidal,[d] Adel Kadri,[e,f] Kaïss Aouadi[a,b*]

[a]University of Monastir, Faculty of Sciences of Monastir, Laboratory of Heterocyclic Chemistry, Natural Products and Reactivity, Avenue of the Environment, 5019 Monastir, Tunisia.

[b]Department of Chemistry, College of Science, Qassim University, Buraidah 51452, Saudi Arabia

[c] Carthage University, Faculty of Sciences of Bizerte, 7021 Jarzouna, Tunisia

[d] Université Claude Bernard Lyon 1, Université de Lyon, Institut de Chimie et Biochimie Moléculaires et Supramoléculaires, UMR CNRS 5246, Laboratoire de Chimie Organique 2-Glycochimie, Bâtiment Lederer, 1 Rue Victor Grignard, F-69622 Villeurbanne, France.

[e] Faculty of Science of Sfax, Department of Chemistry, Sfax University, B.P. 1171, 3000 Sfax, Tunisia.

[f]College of Science and Arts in Baljurashi, Albaha University, P.O. Box (1988). Albaha, Saudi Arabia.

[*]Corresponding author:

Kaïss Aouadi; Kaiss_aouadi@hotmail.com

Abstract

A series of novel isoxazolidines based on benzaldehyde derivatives have been synthesized from the cycloaddition of chiral menthone-based nitrone and allyl phenyl ethers. All synthetic compounds were assessed for their *in vitro* PPA, HPA and HLAG inhibitory activity. The results revealed that all targets exhibited better inhibitory effect against PPA ($12.3 < IC_{50} < 38.2$ μM), HPA ($10.1\pm0.4 < IC_{50} < 26.8\pm0.2$ μM) and HLAG ($65.4\pm1.2 < IC_{50} < 274.8\pm1.1$μM) when compared with the reference inhibitor, acarbose (IC_{50}=284.6±0.3 μM for PPA, 296.6±0.8 μM for HPA, 780.4±0.3 μM for HLAG) with the highest PPA inhibitory activity was ascribed to compound **3g** against both PPA and HPA, and 3b against HLAG enzymes, respectively. Structural activity relationships (SARs) were also established for all synthesized compounds and the interaction modes of the most potent inhibitor (**3g**) and the active site with residues of three enzymes were confirmed through molecular docking studies. Furthermore, a combination of molecular docking analysis with the *in vitro* activities can help to improve prediction success and encourages the uses of some of these molecules as potential alternatives toward the modulation of T2D.

Keywords: 1,3-dipolar cycloaddition, nitrone, isoxazolidine, porcine and human pancreatic α-amylase activity, α-glucosidase activity, molecular docking.

Introduction

Diabetes syndrome is a life-threatening and chronic endocrine disease which causes type 1 (T1D, insulin-dependent), type 2 (T2D, noninsulin-dependent) and gestational (GDM, pregnancy) diabetes mellitus (DM), and is characterized by hyperglycemia (defect in insulin secretion, insulin action or both). According to the estimates from the International Diabetes Federation (IDF), the global diabetes prevalence in 2019 will be 9.3% (463 million people), rising to 10.2% (578 million) by 2030 and 10.9% (700 million) by 2045 [1]. Also, 50.1% of people living with diabetes do not know that they have diabetes with the global prevalence of impaired glucose tolerance was estimated to be 7.5% (374 million) in 2019 and projected to reach 8.0% (454 million) by 2030 and 8.6% (548 million) by 2045 with T2D as the predominant form (around 90%) [1-2]. Therefore, to avoid diabetes complications it is necessary to decrease the postprandial hyperglycemia (PPHG) by targeting α-amylase (depolymerizing of long chain carbohydrates) and α-glucosidase (depolymerizing starch and disaccharides into glucose) enzymes which are involved in the digestion of carbohydrates [3]. Acarbose was considered for

a long time as the most widely prescribed α-amylase and α-glucosidase inhibitors to control PPHG, however the administration of this drug is associated with a panel of chronic complications such as gastrointestinal problems, abdominal distention, flatulence and diarrhea [4]. Consequently, the research for alternative drug candidates to control glucose levels is crucial for the management of T2DM.

Nitrones have been widely used as precursors for the synthesis of enantiopure organic compounds endowed with important biological activities such as the heterocyclic isoxazolines [5], isoxazolidines [6-9], oxazines [10] derivatives and other natural products [11]. In turn, the isoxazolidine functional group, obtained by 1,3-dipolar cycloaddition between a nitrone and an alkene, plays a crucial role in several chemical transformations due to the lability of the N-O bond [12]. In this context, our research team has been interested for some years in the study of the 1,3-dipolar cycloaddition reaction between chiral nitrones and dipolarophiles to access natural organic compounds such as 4-hydroxyisoleucine [13], 4-hydroxy-L-ornithine [14], and other non-naturally occurring compounds such as 4-hydroxyproline derivatives [15], (αS,3R,4S)-3-glycinyl-4-hydroxypyrrolidine [16] and 4-ylidene (3S)-3-hydroxy-1-aryl (alkyl)-pyrrolidine-2,5-diones [17]. Additionally, the prediction of possible interactions between chemical compounds and the target proteins remains a very important task in research and development process. Also, computational simulations of drug-target interactions using molecular docking as a robust and reliable approach for the prediction of ligand-receptor interactions displayed a crucial role for drug discovery.

In this work, we wish to contribute to expanding the use of chiral nitrone derived from (-)-menthone by synthesizing a new series of polyfunctional isoxazolidines *via* the 1,3-dipolar cycloaddition reaction on various alkenes derived from benzaldehyde. Furthermore, in search of potent anti-diabetic agent, we tried to evaluate their *in vitro* porcine pancreatic α-amylase (PPA), human pancreatic α-amylase (HPA) and human lysosomal acid-α-glucosidase (HLAG) inhibitory effect as well as their *in silico* molecular docking analysis in order to explore the binding interaction of the most potent compound in the active site of the enzyme.

Results and discussion

Allyl phenyl ethers **2a-i** were synthesized by allylation with allyl bromide of the corresponding phenols. The reaction of dipolarophiles **2a-i** with the menthone-based nitrone **1** [18] through 1,3-dipolar cycloaddition provided the cycloadducts **3a-i** with simultaneous creation of two asymmetric centers and with yields ranging from 80 to 92% (Scheme 1). A structure-yield

analysis reveals that higher yields are obtained with the cycloadducts having strong electron donating groups either in the *meta*- (**3h**) or *ortho*-position (**3e-g**) compared to the isoxazolidine part. A lower yield has been obtained for the cycloadduct **3i** having a strong electron donating group (OH) in the *para*-position compared to the compound **3b**. All cycloadducts **3a-i** were obtained with high diastereo- and regioselectivity and their structures determined based on the NMR (1D and 2D) data and a single crystal X-ray diffraction study for compound **3g** [19]. The ^{1}H NMR spectra of compounds **3a-i** clearly indicated that the proton H3 is coupled to H4a with a coupling constant in the range of $J_{3,4a}$ = 6.6 - 8.7 Hz. The coupling constant between H3 and H4b tends to zero. We also found that the coupling constant between protons H5 and H4a ($J_{5,4a}$ > 8 Hz) is greater than that between protons H5 and H4b ($J_{5,4b}$ < 6 Hz). As a result of these observations, and based on literature data for such isoxazolidines [18,20], we can conclude that the H3 / H4a protons are in a *cis* relationship and the H3 / H5 protons are in a *trans* relationship.

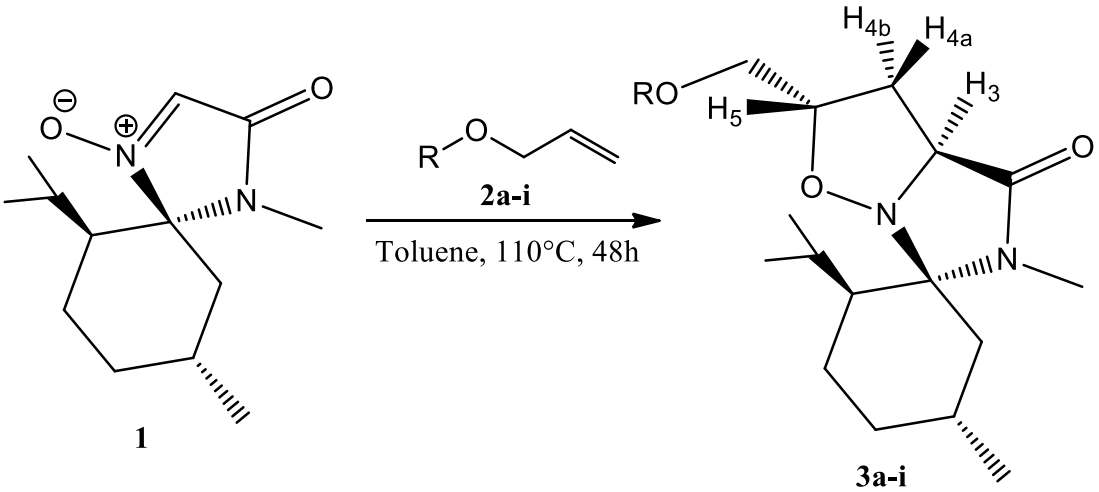

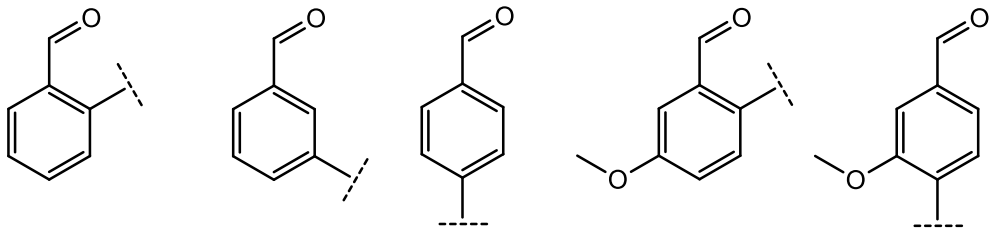

3a, 73% **3b**, 82% **3c**, 77% **3d**, 72% **3e**, 84%

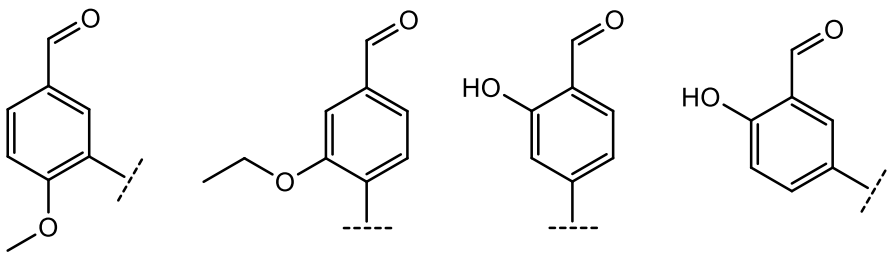

3f, 86% **3g**, 87% **3h**, 86% **3i**, 78%

Scheme 1

Experimental 2D NMR methods such as the NOESY and HMBC were used to further determine the stereo- and regioselectivity of the 1,3-dipolar cycloaddition leading to the **3a-i** cycloadducts. The HMBC spectra of cycloadducts **3a-i** indicated the following significant correlation spots: C=O (imidazolidinone ring) / H4; C6 / H4a; C6 / H4. On the other hand, no correlation could be observed between C6 and H3. These observations confirm the regioselectivity of the 1,3-dipolar cycloaddition reaction between chiral nitrone **1** and dipolarophiles derived from benzaldehyde **2a-i** (Scheme 1).

The NOESY spectrum of compounds **3a-i** shows strong correlations between H3 / H4a protons; H3 / H13; H5 / H4b, and mean intensity correlations between H3 / H14 and H5 / H12b protons. Also, a low intensity correlation was observed between H3 / H4b and H4a / H5 protons. All these observations further confirm the stereochemistry proposed in Figure 1. Moreover, a single-crystal X-ray diffraction study (Figure 2) [19] performed with compound **3g** further and unambiguously confirmed the stereochemistry depicted in the Scheme 1.

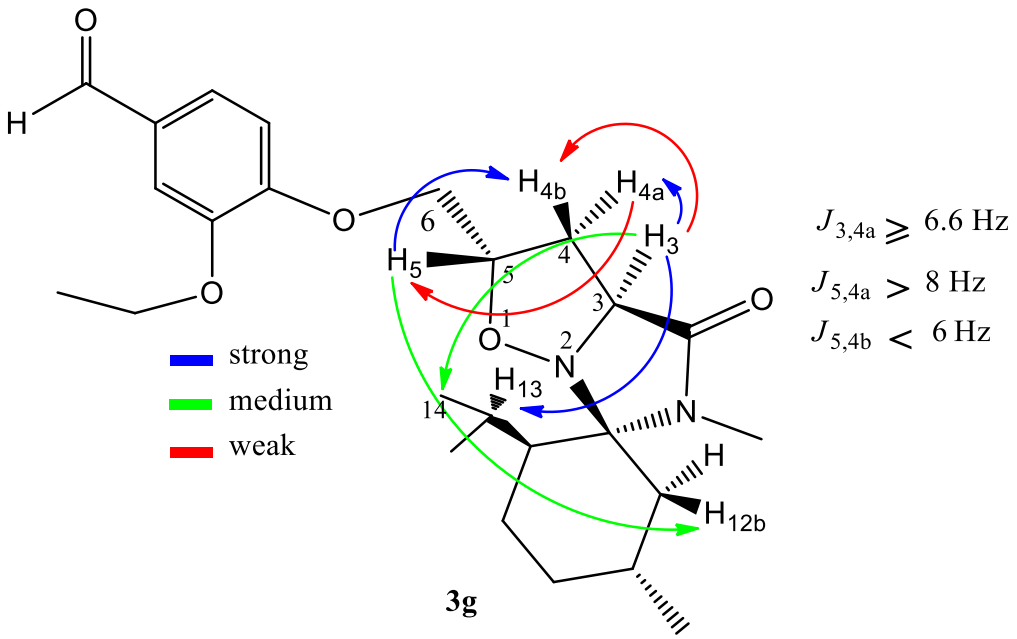

Figure 1

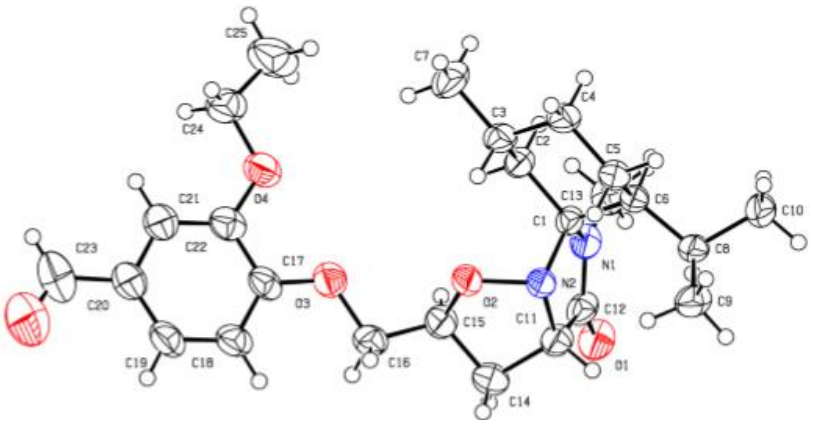

Figure 2

***In vitro* PPA, HPA and HLAG inhibitory effect**

All the prepared derivatives **3a–i** were screened to evaluate their PPA, HPA and HLAG inhibitory. The summarized results in Table 1 showed that all compounds displayed significant activity with IC_{50} values in the range of 12.3-38.2±0.4-0.9 µM, 10.1-26.8±0.2-0.4 µM and 65.4-274.8±1.1-1.2 µM for PPA, HPA and HLAG, respectively in comparison with acarbose(IC_{50} = 284.6±0.3 µM for PPA, 296.6±0.8 µM for HPA, 780.4±0.3 µM for HLAG) known as α-amylase and α-glucosidase inhibitor. Results revealed that all of the synthesized compounds were found to be better inhibitors than acarbose with **3g** followed by **3a** and **3d** as the most potent PPA and HPA inhibitors displaying respectively IC_{50} values of 12.3±0.4 µM and 10.1±0.4 µM (**3g**), 13.8±0.8 and 14.3±0.5 µM (**3a**) and 16.2±0.5 and 15.1±0.2 µM (**3d**). However against HLAG, compounds **3b** (IC_{50}=65.4±1.2 µM), followed by **3i** (87.7±0.8 µM) and **3h** (91.2±1.5 µM) were the most active.

Table 1: *In vitro* PPA, HPA and HLAG inhibitory activities of compounds **3a-i**

Compound	**IC_{50} (µM) of** PPA	**IC_{50} (µM) of** HPA	**IC_{50} (µM) of** HLAG
3a	13.8±0.8	14.3±0.5	130.5±0.8
3b	34.7±0.3	23.5±0.3	65.4±1.2
3c	29.4±0.2	20.6±0.4	113.7±0.7
3d	16.2±0.5	15.1±0.2	208.6±1.0
3e	38.2±0.9	26.8±0.2	184.4±1.3
3f	33.6±0.6	24.2±0.9	155.3±0.8

3g	12.3±0.4	10.1±0.4	274.8±1.1
3h	25.6±0.2	17.3±0.3	91.2±1.5
3i	22.1±0.3	21.4±0.7	87.7±0.8
Acarbose	284.6±0.3	296.6±0.8	780.4±0.3

Structure-Activity Relationships (SARs)

To optimize PPA, HPA and HLAG potential inhibitory activity in relation to electronic influence on enzyme inhibition, SARs study may be investigated based on the above results. As shown, against both PPA and HPA, the most effective compounds **3g**, **3d** and **3a** indicating that addition of methoxy group to the benzaldehyde moiety at the *meta*-position (**3d**) seems to influence slightly the inhibitory effect of α-amylase when compared to **3a** (isoxazolidines in *ortho*- position)**,** however the presence of ethoxy group (**3g)** attached to the benzaldehyde moiety at the *meta*- position in comparison to **3c** (isoxazolidines moiety in the *para*-position) strongly enhanced the α-amylase inhibition, which was confirmed by the observed binding mode suggesting an increase in the closest residues to the docked ligand in the active site (**3g**-PPA, Table 2). Similarly, the methoxylation of **3b** (isoxazolidine moiety in the *meta*- position) in the *para*- position to give **3f** did not influence the activity (IC_{50} = 34.7±0.3 µM for **3b** *vs.* 33.6±0.6 µM for **3f**) suggesting the poorly effect of methoxy group, results were confirmed by their equipotent docking score (-7.5 kcal mol^{-1}). Additionally and as mentioned above, the position of the substituted isoxazolidine moiety (*ortho*-position) in **3a** followed by **3b** (*para*-position) and **3c** (*meta*-position) on the benzaldehyde moiety displayed a strong influence on α-amylase inhibition, which allows to confirm that the activity is due in major part to the isoxazolidine part. If we compare compounds **3h** (IC_{50} = 25.6±0.2 µM) and **3i** (IC_{50} = 22.1±0.3 µM) containing hydroxyl group at the *ortho*- position with those **3c** (IC_{50} = 29.4±0.2 µM) and **3b** (IC_{50} = 34.7±0.3 µM)**,** respectively**,** we note that the highest inhibitory potential of these compounds may be due to the donating electron effect of hydroxyl group. It is interesting to point out that introduction of methoxy group at the *meta*-position having withdrawing effect in **3e** compared to **3c** decreased the inhibition towards α-amylase.

The great inhibitory potential of **3b** (IC_{50} = 65.4±1.2 µM) against HLAG could be due to the presence of electron-withdrawing isoxazolidine group (*meta*-position) on the benzaldehyde moiety which might enhance the activity in comparison to the *ortho*-isoxazolidine group (**3a,** IC_{50} = 130.5±0.8 µM) and *para*-isoxazolidine group (**3c,** IC_{50} = 113.7±0.7 µM) acting as

electron-donating groups. This was confirmed in **3i** (IC_{50} = 87.7±0.8 μM) by the presence of electron donating substituent OH on the benzaldehyde moiety which decrease also the HLAG activity as compared to **3b** (IC_{50} = 65.4±1.2 μM). Although, a decrease in the inhibitory potential was observed in compounds **3d** and **3e** bearing methoxy group as compared to **3a** and **3c**, respectively as well as when compared to **3g** having ethoxy group (vs. **3c)**, suggesting that the presence of these groups with hindered steric influence negatively the inhibitory potential of our compounds. The same trend was shown with **3f**.

Structure-Based Docking Studies

The potential antidiabetic activity of the tested targets was performed by evaluating their ability to inhibit PPA, HPA and HLAG. Molecular docking studies were carried out using AutoDock Vina software in order (i) to validate and provide the PPA (PDB code: 1HX0), HPA (PDB code: 5E0F) and HLAG (5NN8) inhibitory activities and (ii) to determine the binding modes involved between active binding sites of protein target and our docked synthesized derivatives **3a–i**. The main objective was to identify the best orientation of the ligand in complex with the protein with the overall minimal energy. As per the molecular docking results presented in Table 2, it can be concluded that the lowest binding energy (ΔG) values of compounds **3a** (-8.8 kcal mol^{-1}), **3d** and **3g** (-8.7 kcal mol^{-1}), as well as the highest stability of the ligand-PPA complex are in good accordance with their promising inhibition activity.

Table 2: Docking binding energies (kcal mol^{-1}), number of H-bonds and number of closest residues of the docked compounds 3a-i into the active site of PPA.

Compound	Free binding energy (kcal mol^{-1})	Number of H-bonds	Number of closest residues to the docked ligand in the active site
3a	-8.8	2	19
3b	-7.5	1	13
3c	-7.8	2	12
3d	-8.7	3	21
3e	-7.5	2	11
3f	-7.5	1	14
3g	-8.7	2	21
3h	-7.8	3	11
3i	-8.1	4	12

We then generated a number of possible conformations (poses) of the ligand with a particular dihedral angle within the protein binding site in order to identify the most likely binding

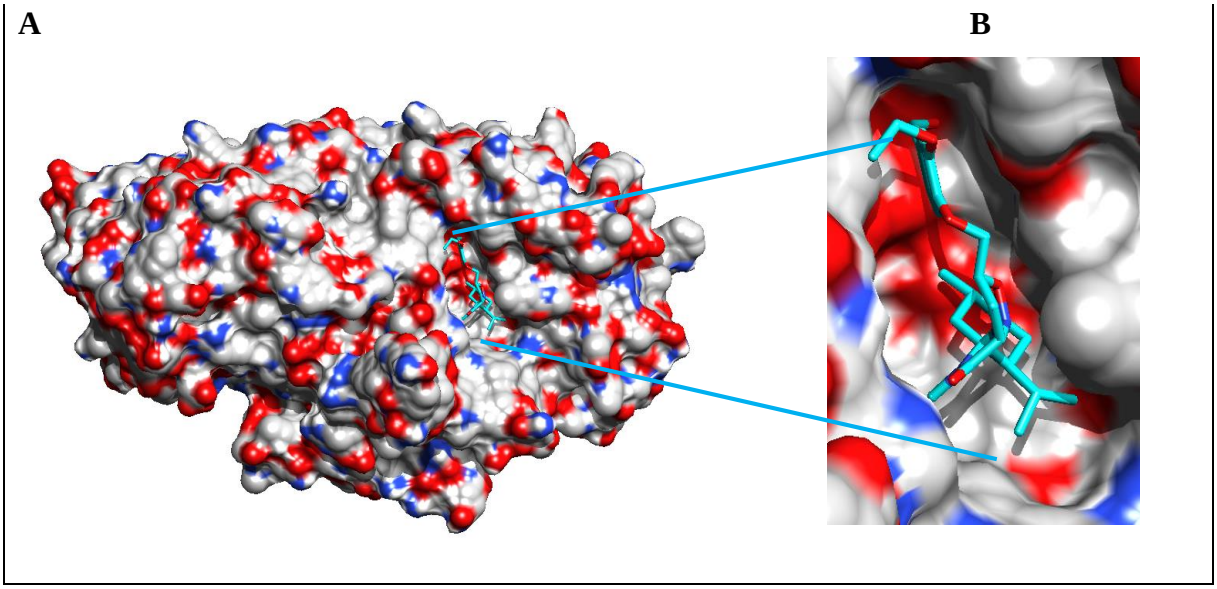

conformations with global minimum on the potential energy surface. Figure 3A provide the surface representation of PPA and the sticks representation (cyan color) of the docked conformation of compound **3g**. this compound fit very well in the active site binding pocket.

This pocket represents, in the original structure, the PPA catalytic site bound to the co-crystallized ligand acarviosine-glucose. In fact, the acarviosine-glucose considered as the smallest compound of the trestatin family that inhibits PPA and nonetheless is not hydrolyzed by the enzyme [21]. Figure 3B show the representation of compound **3g** in its predicted docked conformation with more details. We can see that the rings are positioned in two different sub-pockets that embrace the complete PPA catalytic site. We think that the added benzaldehyde group in this compound contribute to the stabilization of the ligand by its orientation since they fit very well in the pocket facing the solvent and add stabilization to the binding energy found in the rings inside PPA catalytic site [22].

Figure 3. Representation of PPA structure with docking conformation of compound **3g**. (A) Surface representation of PPA and the sticks representation (cyan color) of the docked conformation of compound **3g**. (B) Detailed representation of compound **3g** predicted docked conformation.

In summary, the more favorable predicted binding energy of the conformation **3g**, suggest that this conformation was probably the actual binding modes of this compound.

We have noticed that there is a relationship between the dihedral angle θ plane formed by the atoms 1, 2 and 3 and the plane formed by atoms 2, 3 and 4 (Figure 4A) before docking and the binding energies (ΔG) values for this series of compounds after docking. Values of dihedral angles which are between 145° and 160° have the lowest binding energies and the others with dihedral angles between 80° and 100° have less favorable binding energies. The structures with a dihedral angle between 145° and 160° show that the added groups are found with a smaller distance with the original rings in **3a**, **3d** and **3g** than in the other compounds which suggests the existence of intramolecular interaction between them. This is very interesting because it shows that when we have an intramolecular interaction between the added groups and the rings, we have a dihedral angle (defined by atoms 1, 2, 3 and 4) between 145° and 160° degrees and we predict a better binding energy in the PPA catalytic site. This range of angles seems to give a structure which fits very well in this site. This is confirmed by the IC_{50} values (Figure 4B) which shows a relationship between the dihedral angles and the inhibitory activity.

(A)

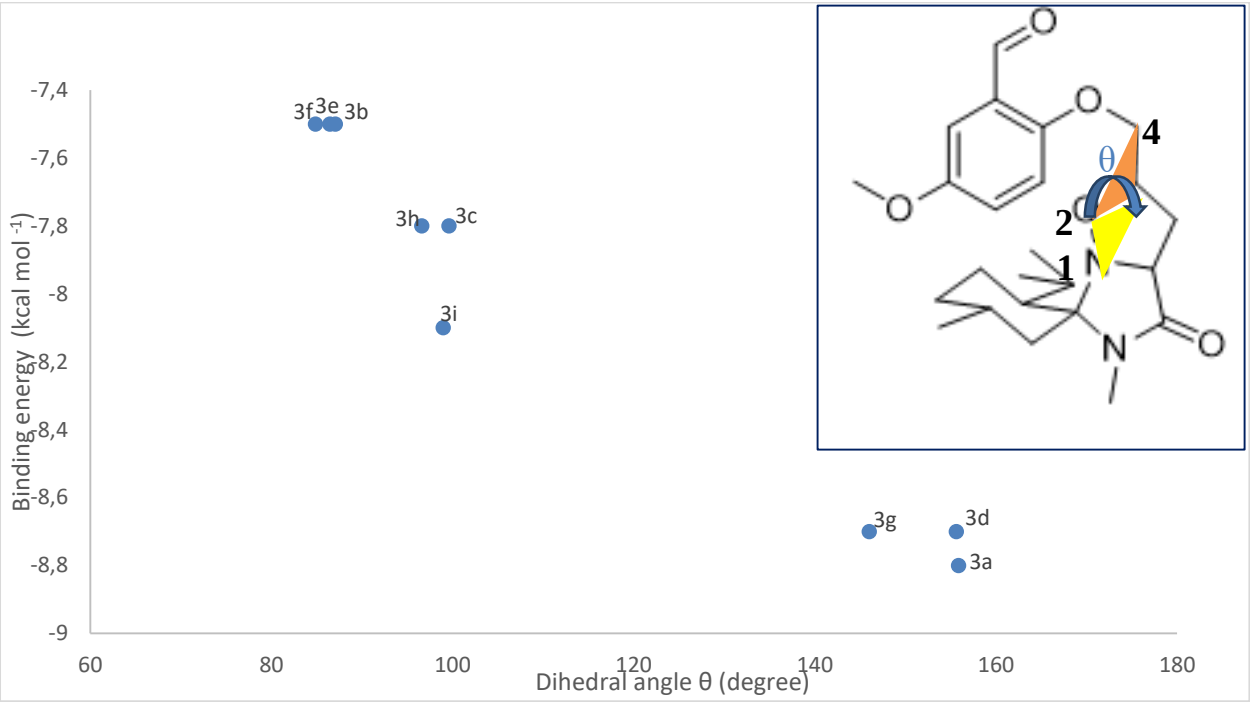

(B)

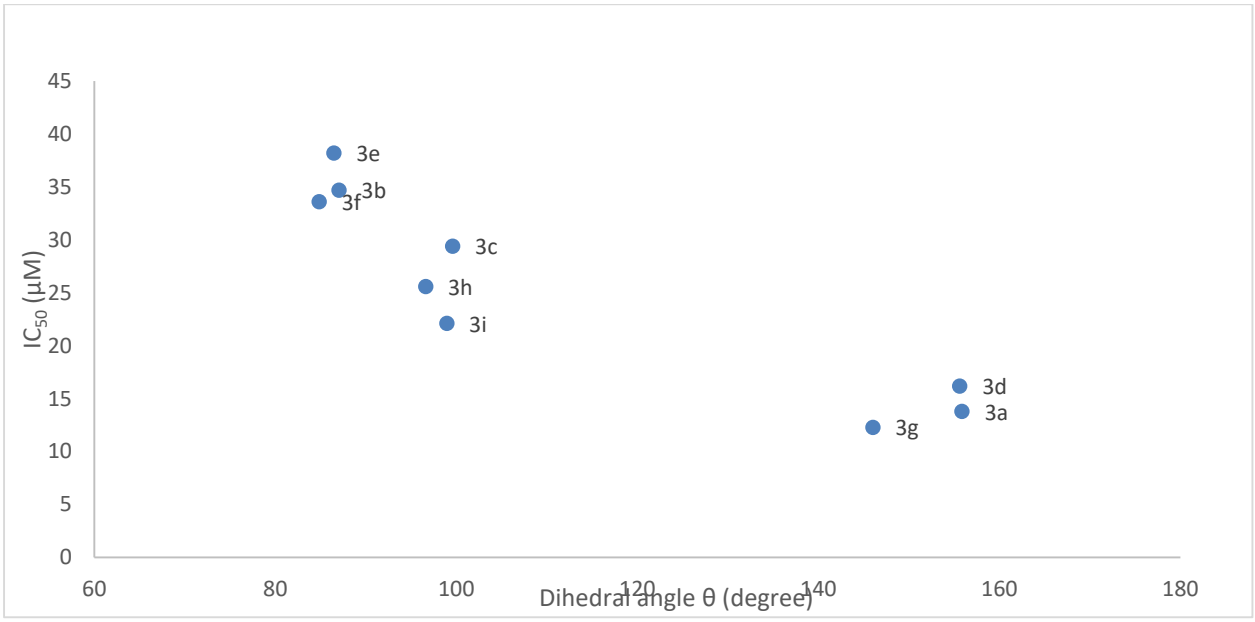

(C)

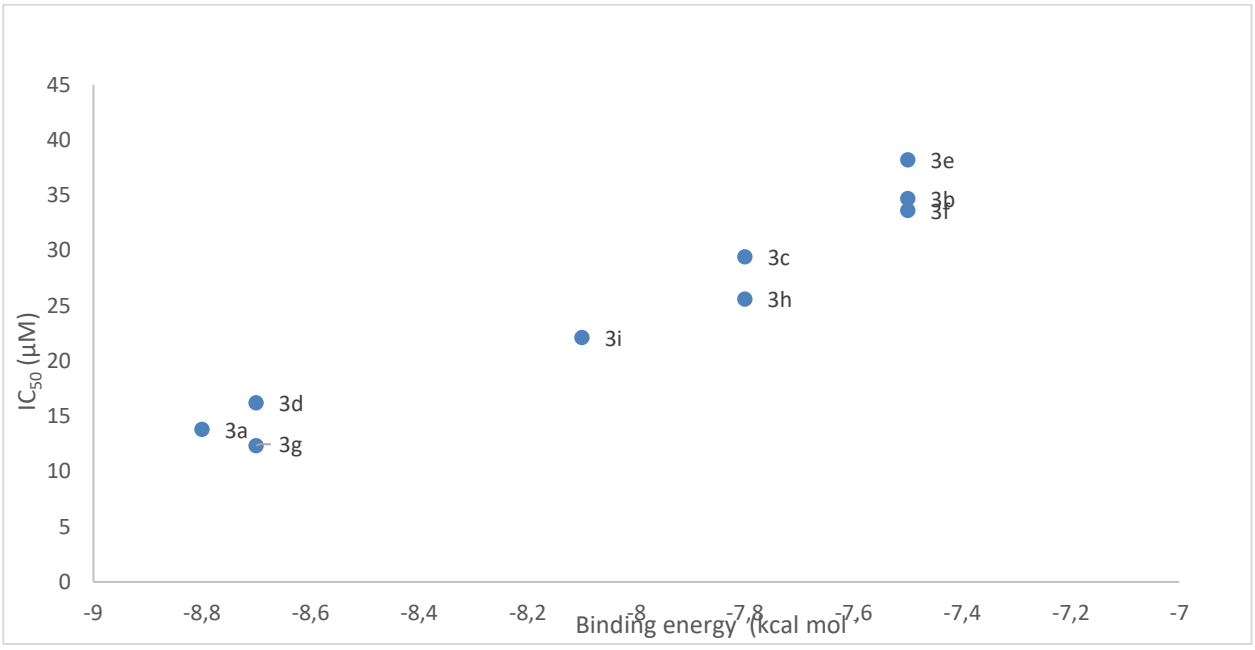

Figure 4. (A) Docking binding energy of compounds **3a-i** in function of the dihedral angle θ (between plane formed by the atoms 1,2 and 3 and the plane formed by atoms 2,3 and 4), (B) IC_{50} (µM) of compounds **3a-i** in function of the dihedral angle θ, (C) IC_{50} (µM) of compounds **3a-i** in function of the Docking binding energy

The docking binding are also in agreement with the IC_{50} values (Figure 4C). All these results prove that **3g**, **3d** and **3a** are the most favorable structures that bind to the active site. It suggests an explanation for our compounds that possess an intramolecular interactions and a certain range of dihedral angles fit better to the catalytic site. To our knowledge, this is the first time

that such an explanation is proposed for the inhibition of this protein and this provide new insights into structure-based design of new inhibitors.

To gain further insights into the interactions mode of the most potent compound **3g** in the active site of PPA and explain the related inhibitory effect in close relationship with the number of closest residues surrounded the docked compound (Figure 5, Table 2), docking study results PPA showed that **3g** displayed two conventional hydrogen bonding interactions between the oxygen atom of benzaldehyde carbonyl group and Lys200 of 2.43 Å and between the the *oxo* group of isoxazolidine moiety and His305 of 1.97 Å, respectively. Additionally, several interactions (alkyl and Pi-alkyl) can established between isoxazolidine moiety and the PPA active site residues Ala198, Leu162, Val163, Trp53, Leu165, Trp 58, as well as two carbon hydrogen bond interactions between methyl group attached to the nitrogen atom of isoxazolidine moiety and Asp300 and between the hydrogen of benzaldehyde carbonyl group and His201 interactions, respectively. Also, the interactions involved in the phenyl ring of **3g** are carbon hydrogen bond with His201 of 3.7 Å, and π-alkyl with Lys200, π-sigma with Ile235 of 3.61 Å and π-cation with His201 of 2.77 Å which are responsible of the enhanced stability in **3g**-PPA complex as well as the hydrophobic contacts between benzaldehyde moiety and Ala307, Tyr151, Ser199, Val234, Glu233 and Gly306 residues (Figure 6). Taking into account of all these interaction modes, we can confirm the higher stability the **3g**-PPA (-8.7 kcal mol^{-1}) and its strongest inhibitory effect.

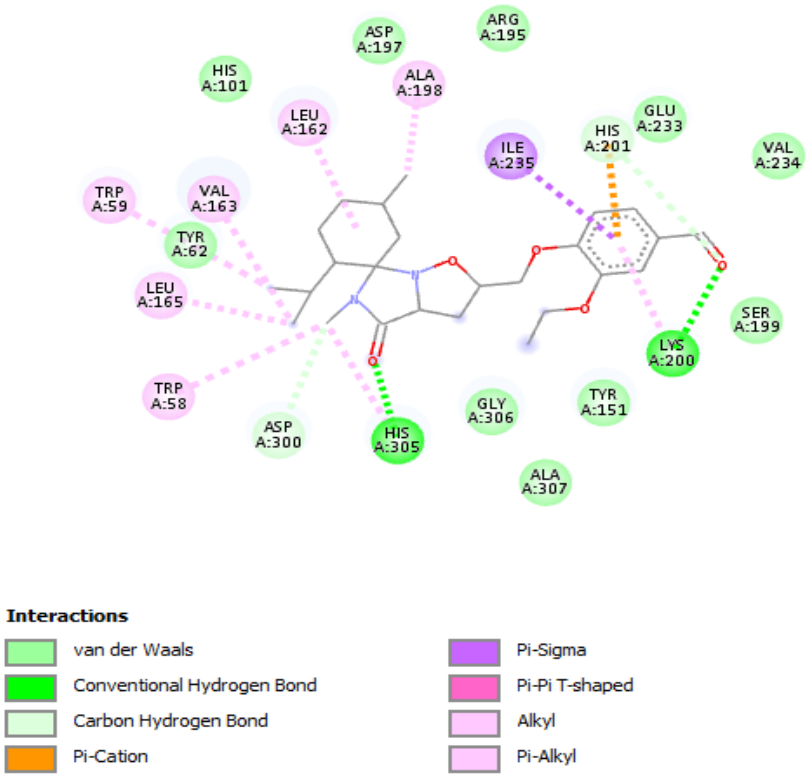

Figure 5: 2D of the closest interactions between the active site residues of PPA and the most potent compound **3g**.

Regarding the results depicted in Table 3, all the stable complexes formed between the docked isoxazolidine derivatives and HPA exhibited better or equipotent negative binding energy as compared to PPA complexes suggesting that they are thermodynamically better inhibited by HPA. It was clear from the docking results that compounds **3a, 3d and 3g** having the highest inhibitory activity (IC_{50}) were found to be the most potent and strongly bounded into the active site (-8.8 $kcal.mol^{-1}$). The binding interactions (Table 3 and Figure 6) indicated that **3g**-HPA formed one conventional hydrogen bond between the oxygen atom of benzaldehyde carbonyl group and Ile235 of 2.30 Å. Moreover, hydrophobic interactions have been established between the aromatic ring and Ile235 of 3.85 Å (Pi-sigma) and His201 of 3.66 Å (Pi-cation) which maintained the improved potency and the stability of the **3g**-HPA complex. Also, the HPA residues Leu162 of 5.14 Å and Ala198 of 5.03 Å showed π-alkyl interactions with the aromatic ring, however the isoxazolidine moiety was bounded to HPA residues by eight hydrophobic interactions (seven π-alkyl and one π-sigma). Moreover, the presence of hydrophobic interactions the surrounding the complex **3g**-HPA such as Tyr151, Val234, Lys200, Glu233, Asp197, His101, Thr163, Leu165 residues enhanced the stability of the complex (Figure 6).

Table 3: Docking binding energies (kcal mol^{-1}), number of H-bonds and number of closest residues of the docked compounds **3a-i** into the active site of HPA.

Compound	Free binding energy (kcal mol^{-1})	Number of H-bonds	Number of closest residues to the docked ligand in the active site
3a	-8.8	0	15
3b	-8.5	1	16
3c	-8.5	1	16
3d	-8.8	0	16
3e	-8.3	1	17
3f	-8.1	3	16
3g	-8.8	1	18
3h	-8.7	2	17
3i	-8.4	1	16

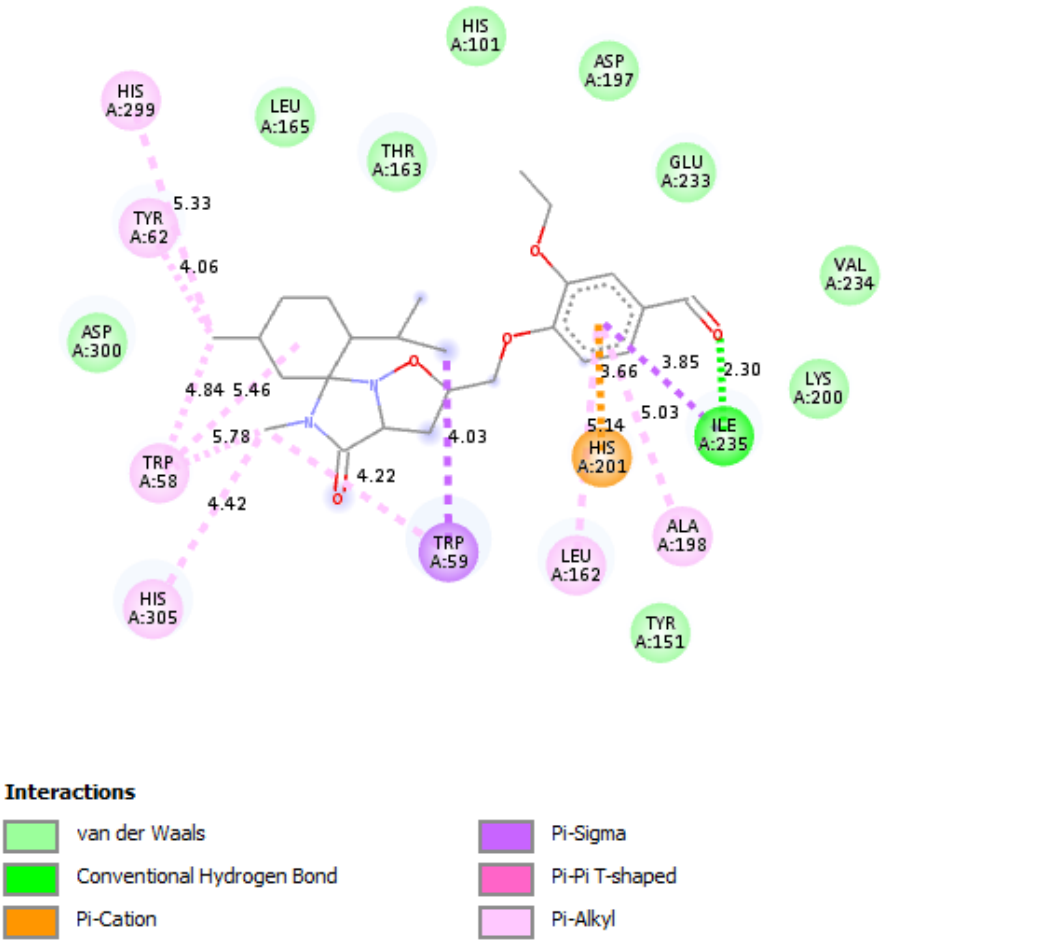

Figure 6: 2D of the closest interactions between the active site residues of HPA and the most potent compound **3g**.

Providing the X-ray crystal structure and enzyme kinetics studies on α-amylase, it has been demonstrated that the active site of α-amylase contain three important residues namely Asp197, Glu233 and Asp300 [23-24]. Their mechanism of action on the hydrolysis of polymeric substrates such as starch was conducted as follows: Asp197 acts as a nucleophile, however Glu233 intervenes in acid-base catalysis during the hydrolysis reaction and Asp300 play a role in optimizing the orientation of the substrate. Williams et al., [23] using myricetin as an inhibitor for α-amylase, they found that it can binds at the active site of α-amylase *via* four hydrogen bond interactions with Gln63, His101and Asp197 and two hydrophobic interactions with Tyr62 and Leu165, respectively. Also, several amino acid residues such as Trp59, Val98, Leu162, Val163, Ala198, and Glu233 can stabilize more the myricetin α-amylase complex. As shown in Figure 6, our docking results are well correlated with this finding, suggesting that compound **3g** was well bounded at the active site of both α-amylase (PPA and HPA) at a place close to the binding site of myricetin with also the presence of the important 3 residues (Asp197, Glu233 and Asp300) of the active site.

The docking result of our synthesized compound in the active site of α-glucosidase enzyme showed that the binding energy values ranged from -7.8 to -7.0 kcal mol^{-1} with **3b** having the potent inhibitory activity and fits perfectly at the enzyme active site (Table 4, Figure 7). **3b**-HLAG complex was stabilized by the establishment of one conventional hydrogen bond interactions between the oxygen atom of benzaldehyde carbonyl group and His674 of 2.59 Å. Additionally, the aromatic ring involved π-anion and π-π stacking interactions between Asp518 of 3.81 Å and Phe649 of 5.25 Å, respectively. The isoxazolidine moiety interacted with HPA residues *via* one carbon hydrogen bond interactions (Asp616) and several alkyl and π-alkyl interactions. Furthermore, the complex was also stabilized by the presence of hydrophobic contacts of the benzaldehyde moiety with Trp481, Trp613, Trp516, Arg672, Asp404, Ile441 residues (Figure 7).

Table 4: Docking binding energies (kcal mol^{-1}), number of H-bonds and number of closest residues to the docked compounds **3a-i** into the active site of HLAG.

Compound	Free binding energy (kcal mol^{-1})	Number of H-bonds	Number of closest residues to the docked ligand in the active site
3a	-7.4	1	17

3b	-7.8	1	15
3c	-7.3	1	14
3d	-7.1	1	19
3e	-7.0	0	17
3f	-7.1	2	18
3g	-7.0	1	13
3h	-7.6	3	14
3i	-7.6	3	18

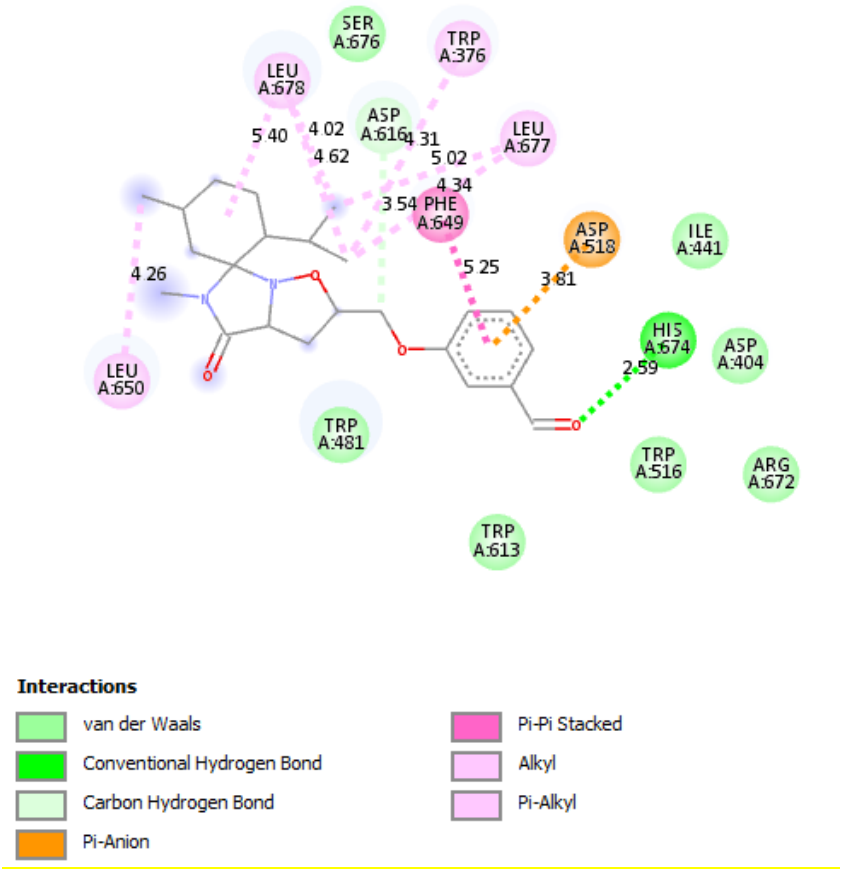

Figure 7: 2D of the closest interactions between the active site residues of HLAG and the most potent compound **3b**.

Based on the work of Roig-Zamboni *et al.* [25] on the X-ray crystal structure of HLAG enzyme with 1-deoxynojirimycin and its derivative *N*-hydroxyethyl-deoxynojirimycin, it has been found that the amino-sugar, 1-deoxynojirimycin as a good inhibitor of α-glucosidase can stabilize the active site of α-glucosidase through hydrogen bonds (Asp404, Asp518, Arg600, Asp616, and His674) and hydrophobic interactions (Trp376, Ile441, Trp516, Met519, Trp613, and Phe649) [25]. Also, the α-glucosidase residues that can interact with 1-deoxynojirimycin

are Leu405, Trp481, Asp645, and Arg672 [25]. Additionally, the presence of two active site residues namely Asp518 and Asp616 mainly act as a catalytic nucleophile and acid/base respectively in the classical Koshland double displacement reaction mechanism [25]. This is in good agreement with our docking results confirming that **3b** was well bounded at the active site of α-glucosidase and interacting with many amino acid residues that are involved in the stability of 1-deoxynojirimycin/α-glucosidase complex (Figure 7).

Conclusion

In summary, we have successfully designed and synthesized a novel class of antidiabetic targets with isoxazolidines derivatives from a readily available chiral nitrone and simple allyl phenyl ethers through a 1,3-dipolar cycloaddition. The cycloadducts were evaluated for their inhibitory properties against PPA. A significant inhibitory activity was found for all the examined compounds with IC_{50} values about 7-23 folds lower than that of acarbose. Additionally, molecular docking was performed on the active site of PPA, HPA and HLAG enzymes and the results provided more insights into the interactions. We noticed the presence a good relationship between: (i) the presence of intramolecular interactions, (ii) their role for the structure to possess a special range of a particular dihedral angle relative to the other complexes with no intramolecular forces. They also confirm respectively, the binding of compound **3g** displaying the strongest inhibitory effect to the active sites of both PPA and HPA as well as **3b** to HLAG active site which reinforces their use as alternate therapeutics for development of antidiabetic agents for the treatment of type 2 diabetes with safety profile. These findings confirm that the interaction of our synthesized compounds with three enzymes as well as the type of substituents depending on their position on the benzaldehyde moiety encourage medicinal chemists to explore a new strategy to develop antidiabetic agents based on isoxazolidines derivatives for high-efficiency PPA, HPA and HLAG inhibition.

Methods

Chemistry

General procedure for the 1,3-dipolar cycloaddition of nitrone to various alkenes 2a-i:

To a solution of nitrone **1** (0.84 mmol, 200 mg, 1 equiv.) in toluene (10 mL) was added alkene **2a-i** (1 equiv). The mixture was heated to reflux during 72h at 110 °C with stirring. TLC showed

the complete conversion of the nitrone. The solution was concentrated, and the residue was purified by flash chromatography (EtOAc/cyclohexane, 3:7) to provide cycloadducts **3a-i**.

3a: 2-(((1S,2S,2'S,3a'S,5R)-2-isopropyl-5,5'-dimethyl-4'-oxotetrahydro-2'H-spiro[cyclohexane-1,6'-imidazo[1,5-b]isoxazol]-2'-yl)methoxy)benzaldehyde

Prepared, according to general procedure, from **1** (1 equiv.) and 2-(allyloxy)benzaldehyde **2a:** (0.84 mmol, 136 mg, 1 equiv.) to afford, after 72h of reaction, **3a** (246 mg, 73%) as a yellow gum. R_f = 0.23 [EtOAc/cyclohexane 4:6]. $[\alpha]_D^{23.9}$ = +27.3 (c = 1, CH_2Cl_2). ^{1}H NMR ($CDCl_3$, 300 MHz): 0.80 (d, 3H, *J* = 6.6 Hz, CH_3), 0.82 (d, 3H, *J* = 6.9 Hz, CH_3), 0.84 (d, 3H, *J* = 6.3 Hz, CH_3), 0.89 (m, 1H), 1.21 (t, 1H, *J* = 6 Hz), 1.31 (m, 1H), 1.41(m, 1H), 1.56 (dd, 1H, *J* = 13.8 Hz, *J* = 3.6 Hz), 1.65 (dd, 1H, *J* = 12.6 Hz, *J* = 2.4 Hz), 1.74 (m, 1H), 1.90 (m, 1H), 2.01 (dt, 1H, *J* = 12.6 Hz, *J* = 2.7 Hz), 2.32 (m,1H), 2.72 (s, 3H, *N*CH_3), 2.76 (ddd, 1H, J = 12.6 Hz, *J* = 5.7 Hz, *J* = 1.5 Hz), 3.98 (d, 1H, *J* = 8.7 Hz), 4.13 (dd, 1H, *J* = 10.2 Hz, J = 6.9 Hz),4.17 (dd, 1H, *J* = 10.5 Hz, *J* = 4.2 Hz), 4.27 (m, 1H), 6.97 (m, 1H),7.00 (t, 1H, *J* = 7.5 Hz), 7.49 (ddd, 1H, *J* = 9 Hz, *J* = 7.2 Hz, *J* = 1.8 Hz), 7.79 (dd, 1H, *J* = 7.8 Hz, *J* = 1.8 Hz), 10.45 (s, 1H). ^{13}C NMR ($CDCl_3$, 75 MHz): *δ* 18.4; 22.1; 22.2; 24.0; 24.2; 26.0; 29.3; 34.5; 35.0; 40.6; 47.9; 65.4; 68.8; 74.8; 89.4; 112.7; 121.1; 125.0; 128.2; 135.7; 160.8; 172.4 (C=O); 189.3 (HC=O). **HRMS**, (**ESI**) calcd $C_{23}H_{32}N_2NaO_4$ $[M+Na]^+$: 423.2260, found 423.2254.

3b: 3-(((1S,2S,2'S,3a'S,5R)-2-isopropyl-5,5'-dimethyl-4'-oxotetrahydro-2'H-spiro[cyclohexane-1,6'-imidazo[1,5-b]isoxazol]-2'-yl)methoxy)benzaldehyde

Prepared, according to general procedure, from **1** (1 equiv.) and 3-(allyloxy)benzaldehyde **2b:** (0.84 mmol, 136 mg, 1 equiv.) to afford, after 72h of reaction, **3b** (276 mg, 82%) as a yellow gum. R_f = 0.19 [EtOAc/cyclohexane 4:6]. $[\alpha]_D^{24}$ = +23 (c = 1, CH_2Cl_2). ^{1}H NMR ($CDCl_3$, 300 MHz): *δ* 0.83 (d, 3H, *J* = 6.9 Hz, CH_3), 0.86 (d, 3H, *J* = 7.5 Hz, CH_3), 0.88 (d, 3H, *J* = 6.9 Hz, CH_3), 0.92 (m, 1H), 1.25 (t, 1H, *J* = 12 Hz), 1.37 (dd, 1H, *J* = 12 Hz, *J* = 3 Hz), 1.45 (dd, 1H, *J* = 12.9 Hz, *J* = 6 Hz), 1.67 (m, 1H), 1.70 (dd, 1H, *J* = 12.3 Hz, *J* =3 Hz), 1.79 (m, 1H), 1.96 (m, 1H), 2.06 (dt, 1H, *J* =12.6 Hz, *J* = 3Hz), 2.34 (ddd, 1H, *J* = 16.8 Hz, *J* = 8.7 Hz, *J* = 7.8 Hz), 2.75 (s, 3H, *N*CH_3), 2.72 (ddd, 1H, *J* = 12.6 Hz, *J* = 5.7 Hz, *J* = 1.5 Hz), 4.01 (d, 1H, *J* = 8.7 Hz), 4.08 (dd, 1H, *J* = 10.2 Hz, *J* = 4.8 Hz), 4.14 (dd, 1H, *J* = 10.2 Hz, *J* = 6), 4.24 (m, 1H), 7.19 (ddd, 1H, *J* = 7.5 Hz, *J* = 2.7 Hz, *J* = 1.8 Hz), 7.39 (t, 1H, *J* = 1.5 Hz), 7.45 (m, 2H), 9.97 (s, 1H). ^{13}C NMR ($CDCl_3$, 75 MHz): *δ* 18.5; 22.3; 22.3; 24.1; 24.4; 26.0; 29.3; 34.6; 35.1; 40.7; 48.1; 65.5; 68.3; 74.9; 89.4; 112.9; 122.1; 123.8; 130.1; 137.7; 159.2; 172.8 (C=O); 192 (HC=O). **HRMS**, (**ESI**) calcd $C_{23}H_{32}N_2NaO_4$ $[M+Na]^+$: 423.2260, found 423.2254.

3c: 4-(((1S,2S,2'S,3a'S,5R)-2-isopropyl-5,5'-dimethyl-4'-oxotetrahydro-2'H-spiro[cyclohexane-1,6'-imidazo[1,5-b]isoxazol]-2'-yl)methoxy)benzaldehyde
Prepared, according to general procedure, from **1** (1 equiv.) and 4-(allyloxy)benzaldehyde **2c:** (0.84 mmol, 136 mg, 1 equiv.) to afford, after 72h of reaction, **3c** (259 mg, 77%) as a yellow gum. R_f = 0.19 [EtOAc/cyclohexane 4:6]. $[\alpha]_D^{23.9}$ = +11.7 (c = 1, CH_2Cl_2). ^{1}H NMR ($CDCl_3$, 300 MHz): 0.84 (m, 9H), 0.92 (m, 1H), 1.25 (m, 1H), 1.37 (dd, 1H, *J* = 9Hz, *J* = 2.4 Hz),1.44 (dd, 1H, *J* = 10.2 Hz, *J* = 5.1 Hz), 1.61 (ddd, 1H, *J* = 11.7 Hz, *J* = 6.3 Hz, *J* = 2.7 Hz), 1.69 (dd, 1H, *J* = 9.6 Hz, *J* = 2.4Hz), 1.78 (m, 1H), 1.93 (m, 1H), 2.04 (dt, 1H, *J* = 9.6 Hz, *J* = 1.8 Hz), 2.38 (m, 1H), 2.75 (s, 3H, *N*CH_3), 2.78 (ddd, 1H, *J* = 9.3 Hz, *J* = 4.2 Hz, J = 1.2 Hz), 4.00 (d, 1H, *J* = 6.6 Hz), 4.11 (dd, 1H, *J* = 7.8 Hz, *J* = 3 Hz), 4.17 (dd, 1H, *J* = 7.8 Hz, *J* = 4.8 Hz), 4.24 (m, 1H), 7.01 (d, 2H, *J* = 6.3 Hz), 7.82 (d, 2H, *J* = 6.6 Hz), 9.88 (s, 1H). ^{13}C NMR ($CDCl_3$, 75 MHz): δ 18.4; 22.2; 22.3 (CH_2); 24.1; 24.3; 26.0; 29.3; 34.5 (CH_2); 35.1 (CH_2); 40.6 (CH_2); 48.0; 65.5; 68.3 (CH_2); 74.8; 89.4; 114.9; 130.2; 131.9; 163.5; 172.6 (C=O); 190.7 (HC=O). **HRMS**, (**ESI**) calcd $C_{23}H_{32}N_2NaO_4$ $[M+Na]^+$: 423.2257, found 423.2254.

3d: 2-(((1S,2S,2'S,3a'S,5R)-2-isopropyl-5,5'-dimethyl-4'-oxotetrahydro-2'H-spiro[cyclohexane-1,6'-imidazo[1,5-b]isoxazol]-2'-yl)methoxy)-5-methoxybenzaldehyde

Prepared, according to general procedure, from **1** (1 equiv.) and 2-(allyloxy)-5-methoxybenzaldehyde **2d:** (0.84 mmol, 161 mg, 1 equiv.) to afford, after 72 h of reaction, **3d** (260 mg, 72%) as a yellow oil. R_f = 0.23 [EtOAc/cyclohexane 4:6]. $[\alpha]_D^{23.9}$ = +25.4 (c = 1, CH_2Cl_2). ^{1}H NMR ($CDCl_3$, 300 MHz): δ 0.82 (d, 3H, *J* = 6.6 Hz, CH_3), 0.85 (d, 3H, *J* = 6.9 Hz, CH_3), 0.87 (d, 3H, *J* = 6.6 Hz, CH_3), 0.93 (m, 1H), 1.25 (m, 2H), 1.36 (m, 1H), 1.65 (m, 2H), 1.78 (m, 1H), 1.92 (m, 1H), 2.03 (dt, 1H, *J* = 12.6 Hz, *J* = 3 Hz), 2.32 (ddd, 1H, *J* = 17.7 Hz, *J* = 9 Hz, *J* = 2.7 Hz), 2.75 (s, 3H, *N*CH_3), 2.77 (ddd, 1H, *J* = 12.3 Hz, *J* = 5.7 Hz, *J* = 1.5 Hz), 3.79 (s, 3H, OCH_3), 3.99 (d, 1H, *J* = 8.7 Hz), 4.10 (dd, 1H, *J* = 10.5 Hz, *J* = 6.9 Hz), 4.15 (dd, 1H, *J* = 10.5 Hz, *J* = 3.9 Hz),4.27 (m, 1H), 6.95 (d, 1H, *J* = 9 Hz), 7.10 (dd, 1H, *J* = 9 Hz, *J* = 3.3 Hz), 7.31 (d, 1H, *J* = 3 Hz), 10.44 (s, 1H). ^{13}C NMR ($CDCl_3$, 75 MHz): δ 18,4; 22,3; 22,3 (CH_2); 24.1; 24.3; 26.0; 29.4; 34.6 (CH_2); 35.0 (CH_2); 40.7 (CH_2); 48.1; 55.8; 65.5; 69.8 (CH_2); 75.0; 89.5; 110.1; 114.9; 123.4; 125.4; 154.0; 155.7; 172.5 (C=O); 189.2 (HC=O). **HRMS**, (**ESI**) calcd $C_{24}H_{34}N_2NaO_5$ $[M+Na]^+$: 453.2365 found 453.2360.

3e: 4-(((1S,2S,2'S,3a'S,5R)-2-isopropyl-5,5'-dimethyl-4'-oxotetrahydro-2'H-spiro[cyclohexane-1,6'-imidazo[1,5-b]isoxazol]-2'-yl)methoxy)-3-methoxybenzaldehyde

Prepared, according to general procedure, from **1** (1 equiv.) and 4-(allyloxy)-3-methoxybenzaldehyde **2e:** (0.84 mmol, 161 mg, 1 equiv.) to afford, after 72h of reaction, **3e**

(304 mg, 84%) as a yellow oil. R_f = 0.17 [EtOAc/cyclohexane 4:6]. $[\alpha]_D^{24.3}$ = +9.1 (c = 1, CH_2Cl_2). ^{1}H NMR ($CDCl_3$, 300 MHz): δ 0.83 (d, 3H, *J* = 6.9 Hz, CH_3), 0.84 (d, 3H, *J* = 6.6 Hz, CH_3), 0.85 (d, 3H, *J* = 6.9 Hz, CH_3), 0.91 (m, 1H), 1.23 (m, 1H), 1.36 (m, 1H), 1.43 (m, 1H), 1.66 (td, 2H, *J* = 15.9 Hz, *J* = 3.6 Hz), 1.78 (m, 1H), 1.93 (m, 1H), 2.04 (dt, 1H, *J* = 12.6 Hz, *J* = 2.7 Hz), 2.38 (ddd, 1H, *J* = 17.1 Hz, *J* = 9 Hz, *J* = 8.1 Hz), 2.74 (s, 3H, *N*CH_3), 2.80 (ddd, 1H, *J* = 12.3 Hz, J = 5.4 Hz, *J* = 1.5 Hz), 3.90 (s, 3H, OCH_3), 4.00 (d, 1H, *J* = 8.7 Hz), 4.18 (dd, 1H, *J* = 10.5 Hz, *J* = 5.1 Hz), 4.22 (m, 1H), 4.30 (m, 1H), 7.04 (d, 1H, *J* = 8.1 Hz), 7.42 (m, 2H), 9.85 (s, 1H). ^{13}C NMR ($CDCl_3$, 75 MHz): δ 18,4; 22,1; 22,3 (CH_2); 24.1; 24.3; 26.0; 29.3; 34.6 (CH_2); 35.4 (CH_2); 40.6 (CH_2); 48.1; 56.0; 65.5; 69.3 (CH_2); 75.1; 89.4; 109.6; 112.3; 126.4; 130.5; 150.0; 153.6; 172.6 (C=O); 190.9 (HC=O). **HRMS**, (**ESI**) calcd $C_{24}H_{34}N_2NaO_5$ $[M+Na]^+$: 453.2367, Found 453.2360.

3f: 3-(((1S,2S,2'S,3a'S,5R)-2-isopropyl-5,5'-dimethyl-4'-oxotetrahydro-2'H-spiro[cyclohexane-1,6'-imidazo[1,5-b]isoxazol]-2'-yl)methoxy)-4-methoxybenzaldehyde
Prepared, according to general procedure, from **1** (1 equiv.) and 3-(allyloxy)-4-methoxybenzaldehyde **2f:** (0.84 mmol, 161 mg, 1 equiv.) to afford, after 72h of reaction, **3g** (311 mg, 86%) as a yellow gum. R_f = 0.23 [EtOAc/cyclohexan 4:6]. $[\alpha]_D^{23.8}$ = +16.2 (c = 1, CH_2Cl_2). ^{1}H NMR ($CDCl_3$, 300 MHz): δ 0.81 (d, 3H, *J* = 6.6 Hz, CH_3), 0.84 (d, 3H, *J* = 6.9 Hz, CH_3), 0.85 (d, 3H, *J* = 6.6 Hz, CH_3), 0.93 (m, 1H), 1.22 (m,1H), 1.35 (m, 1H), 1.44(m,1H), 1.64 (m, 2H), 1.77 (m, 1H), 1.94 (m, 1H), 2.06 (dt, 1H, *J* = 12.6 Hz, *J* = 2.7 Hz), 2.40 (ddd, 1H, J = 16.8 Hz, J = 9 Hz, J = 7.8 Hz), 2.73 (s, 3H, *N*CH_3), 2.77 (ddd, 1H, *J* = 12.3 Hz, *J* = 5.7 Hz, *J* = 1.5 Hz), 3.92 (s, 3H, OCH_3), 3.98 (d, 1H, *J* = 8.7 Hz), 4.12 (dd, 1H, *J* = 10.8 Hz, *J* = 5.1 Hz), 4.15 (dd, 1H, *J* = 10.5 Hz, *J* = 5.7 Hz), 4.28 (ddd, 1H, *J* = 13.2 Hz, *J* = 7.8 Hz, *J* = 5.4 Hz), 6.96 (d, 1H, *J* = 8.1 Hz), 7.42 (d, 1H, *J* = 2.1 Hz), 7.46 (dd, 1H, *J* = 8.1 Hz, *J* = 1.8 Hz), 9.83 (s,1H). ^{13}C NMR ($CDCl_3$, 75 MHz): δ 18.4; 22.2; 22.3 (CH_2); 24.1; 24.3; 26.0; 29.3; 34.6 (CH_2); 35.3 (CH_2); 40.6 (CH_2); 48.1; 56.0; 65.4; 69.2 (CH_2); 74.8; 89.3; 110.9; 111.3; 126.9; 129.9; 148.7; 154.9; 172.8 (C=O); 190.7 (HC=O). **HRMS**, (**ESI**) calcd $C_{24}H_{34}N_2NaO_5$ $[M+Na]^+$: 453.2363 found 453.2360.

3g: 3-ethoxy-4-(((1S,2S,2'S,3a'S,5R)-2-isopropyl-5,5'-dimethyl-4'-oxotetrahydro-2'H-spiro[cyclohexane-1,6'-imidazo[1,5-b]isoxazol]-2'-yl)methoxy)benzaldehyde
Prepared, according to general procedure, from **1** (1 equiv.) and 4-(allyloxy)-3-ethoxybenzaldehyde **2g:** (0.84 mmol, 173 mg, 1 equiv.) to afford, after 72h of reaction, **3g** (293 mg, 87%) as a yellow gum. R_f = 0.21 [EtOAc/cyclohexane 3:7]. $[\alpha]_D^{23.9}$ = +14.8 (c = 1, CH_2Cl_2). ^{1}H NMR ($CDCl_3$, 300 MHz): δ 0.83 (d, 3H, *J* = 6.6 Hz, CH_3), 0.85 (d, 3H, *J* = 6 Hz, CH_3), 0.86 (d, 3H, *J* = 6.9 Hz, CH_3), 0.91 (m, 1H), 1.25 (t, 1H, *J* = 7.5 Hz), 1.36 (m, 1H), 1.45

(m, 4H), 1.68 (td, 2H, *J* = 12.6 Hz, *J* = 3.6 Hz), 1.78 (m, 1H), 1.92 (m, 1H), 2.04 (dt, 1H, *J* = 12.6 Hz, *J* = 3 Hz), 2.39 (ddd, 1H, *J* = 17.1 Hz, *J* = 9 Hz, *J* = 8.1 Hz), 2.74 (s, 3H, *N*CH_3), 2.79 (ddd, 1H, *J* = 12.3 Hz, *J* = 5.4 Hz, *J* = 1.5 Hz), 4.00 (d, 1H, *J* = 8.7 Hz), 4.13 (q, 2H, *J* = 7.2 Hz, CH_2CH_3), 4.17 (dd, 1H, *J* = 10.5 Hz, *J* = 6 Hz), 4.22 (dd, 1H, *J* = 10.5 Hz, *J* = 6.3 Hz), 4.30 (m, 1H), 7.03 (d, 1H, *J* = 8.4 Hz), 7.40 (m, 2H), 9.84 (s, 1H). ^{13}C NMR ($CDCl_3$, 75 MHz): *δ* 14.7; 18.4; 22.3; 22.3 (CH_2); 24.1; 24.3; 26.0; 29.3; 34.6 (CH_2); 35.4 (CH_2); 40.6 (CH_2); 48.1; 64.5 (CH_2); 65.4; 69.3 (CH_2); 75.1; 89.4; 111.1; 112.8; 126.2; 130.5; 149.1; 154.3; 172.6 (C=O); 190.9 (HC=O). **HRMS**, (**ESI**) calcd $C_{25}H_{36}N_2NaO_5$ $[M+Na]^+$: 467.2517 found 467.2516.

3h: (1S,2S,2'S,3a'S,5R)-2'-((3-hydroxy-4-vinylphenoxy)methyl)-2-isopropyl-5,5'-dimethyldihydro-2'H-spiro[cyclohexane-1,6'-imidazo[1,5-b]isoxazol]-4'(5'H)-one
Prepared, according to general procedure, from **1** (1 equiv.) and 4-(allyloxy)-2-hydroxybenzaldehyde **2h:** (0.84 mmol, 150mg, 1 equiv.) to afford, after 72h of reaction, **3h** (301 mg, 86%) as a yellow gum. R_f = 0.26 [EtOAc/PE 3:7]. $[\alpha]_D^{24.3}$ = +17.9 (c = 1, CH_2Cl_2). ^{1}H NMR (DMSO-d_6, 300 MHz): *δ* 0.79 (d, 3H, *J* = 6.9 Hz, CH_3), 0.80 (d, 3H, *J* = 6.9 Hz, CH_3), 0.82 (d, 3H, *J* = 6.9 Hz, CH_3), 0.92 (m, 1H), 1.29 (t, 1H, *J* = 3.6 Hz), 1.39 (m, 2H), 1.55 (m, 2H), 1.66 (d, 1H, *J* = 12.3 Hz), 1.86 (m, 2H), 2.30 (m, 1H), 2.47 (m, 1H), 2.65 (s, 3H, *N*CH_3), 3.90 (d, 1H, *J* = 8.4 Hz), 4.15 (m, 3H), 6.50 (d, 1H, *J* = 2.4 Hz), 6.58 (dd, 1H, *J* = 8.7 Hz, *J* = 2.1 Hz), 7.62 (d, 1H, *J* = 8.7 Hz), 10.01 (s, 1H), 11.00 (s,1H). ^{13}C NMR (DMSO-d_6, 75 MHz): *δ* 18,6; 22,1; 22,3 (CH_2); 23.9; 24,2; 25,7; 29.1; 34.1 (CH_2); 34,4 (CH_2); 39.9 (CH_2); 47.1; 64.8; 68.1 (CH_2); 74.7; 88.4; 101.7; 107.9; 116.5; 132.0; 163.1; 165.2; 172.0 (C=O); 191.3 (HC=O). **HRMS**, (**ESI**) calcd $C_{23}H_{32}N_2NaO_5$ $[M+Na]^+$: 439.2202 found 439.2203.

3i: 2-hydroxy-4-(((1S,2S,2'S,3a'S,5R)-2-isopropyl-5,5'-dimethyl-4'-oxotetrahydro-2'H-spiro[cyclohexane-1,6'-imidazo[1,5-b]isoxazol]-2'-yl)methoxy)benzaldehyde
Prepared, according to general procedure, from **1** (1 equiv.) and 5-(allyloxy)-2-hydroxybenzaldehyde **2i:** (0.84 mmol, 150 mg, 1 equiv.) to afford, after 72h of reaction, **3i** (273 mg, 78%) as a yellow pate. R_f = 0.12 [EtOAc/PE 3:7]. $[\alpha]_D^{20}$ = +32.1 (c = 1.01, CH_2Cl_2). ^{1}H NMR (DMSO-d_6, 300 MHz): 0.77 (d, 3H, *J* = 7.2 Hz, CH_3), 0.79 (d, 3H, *J* = 7.2 Hz, CH_3), 0.82 (d, 3H, *J* = 6.9 Hz, CH_3), 0.92 (m, 1H), 1.27 (t, 1H, *J* = 6.9 Hz), 1.34 (m, 1H), 1.42 (m, 1H), 1.52 (m, 2H), 1.67 (d, 1H, *J* = 12.6 Hz), 1.78 (m, 1H), 1.89 (d, 1H, *J* = 12.6 Hz), 2.26 (ddd, 1H, *J* = 17.1 Hz, *J* = 12.3 Hz, *J* = 9 Hz), 2.48 (m, 1H), 3.33 (s, 3H, *N*CH_3), 3.89 (d, 1H, *J* = 8.4 Hz), 4.04 (dd, 1H, *J* = 9.9 Hz, *J* = 6.9 Hz), 4.20 (m, 2H), 7.03 (d, 1H, *J* = 2.4 Hz), 7.05 (d, 1H, *J* = 3 Hz), 7.10 (dd, 1H, *J* = 6.9 Hz, *J* = 2.4 Hz), 9.42 (s, 1H), 10.31 (s, 1H). ^{13}C NMR (DMSO-d_6,

75 MHz): δ 18.5; 22.1; 22.2 (CH_2); 24.0; 24.2; 25.8; 29.1; 34.1 (CH_2); 34.5 (CH_2); 47.1; 64.9; 69.8 (CH_2); 74.8; 88.5; 112.0; 116.3; 123.7; 125.3; 151.6; 154.6; 172.0 (C=O); 189.2 (HC=O). **HRMS**, (**ESI**) calcd $C_{23}H_{32}N_2NaO_5$ $[M+Na]^+$: 439.2203, found 439.2203

Molecular Docking

Interactions between derivatives **3a–i** and porcine pancreatic α-amylase (PPA) were studied by *in silico* molecular docking in order to explore the preferred orientation of the ligands in the receptor binding site. We obtained the crystal structure of PPA from the Protein Data Bank (PDB entry: 1HX0). We have removed all the water molecules and the co-crystallized acarviosine-glucose from the structure. Polar hydrogens and Gasteiger charges were assigned with AutoDockTools1.5.2 (ADT) and the PDBQT file format was prepared. [26] ADT was used to select a docking grid, the parameters for X, Y, Z grid center coordinates were 34.0, 20.0, and 53.3, respectively; and the parameters for the X,Y,Z grid dimensions were 30 by 30 by 30 Å. [22]

The structures of compounds **3a-i** were minimized using a conjugate gradient AMMP incorporated in VEGA ZZ. [27] The conversion of the file from PDB to PDBQT was done using ADT. We applied AutoDock Vina software [28] with an exhaustiveness parameter of 32 to perform the docking simulations. ADT was used for the docking conformation analysis. Image preparation was done by chimera [29].

Inhibition assay for α-amylase activity

All compounds were screened for their inhibitory potential against PAA (EC 3.2.1.1) and HPA (EC 3.2.1.1) using the same protocol as described in the literature [22] with slight modification. Acarbose was used as standard. The percent of inhibition was determined by the following formula:

$$\%\ inhibition = \frac{\text{Abs(blank)} - \text{Abs(test compoud)}}{\text{Abs (blank)}} \times 100$$

The results were expressed as IC_{50} (μM) and all the experiments were carried out in triplicates.

Inhibition Assay for α-Glucosidase Activity

α-Glucosidase inhibitory activity was assayed by using 0.1 M phosphate buffer (pH 6.8) at 37°C and the synthesized compounds were dissolved in DMSO (10% final concentration). The enzyme α-glucosidase (EC3.2.1.20, 20 U/mg) in phosphate buffer saline was incubated with

various concentrations of test compounds at 37 °C for 2 min. Then 1.25 mM of substrate (p-nitrophenyl glucopyranoside) was added to the mixture. After further incubation at 37°C for 30 min. the change in absorbance was measured spectrophotometrically at 405 nm. The sample solution was replaced by DMSO as a control. Acarbose was used as a positive control. The percentage of inhibition for each entry was calculated by using the following formula:

$$\%\ inhibition = \frac{\text{Abs(blank)} - \text{Abs(test compoud)}}{\text{Abs (blank)}} \times 100$$

The results were expressed as IC_{50} (µM) and all the experiments were carried out in triplicates.

Acknowledgements

The authors are grateful to the Ministry of Higher Education and Scientific Research of Tunisia for financial support.

References

1. P. Saeedi, I. Petersohn, P. Salpea, B. Malanda, S. Karuranga, N. Unwin , S. Colagiuri, L. Guariguata, A. A. Motala, K. Ogurtsova, J. E. Shaw, D. Bright, R. Williams, Global and regional diabetes prevalence estimates for 2019 and projections for 2030 and 2045: Results from the International Diabetes Federation Diabetes Atlas, 9th edition, DIABETES RESEARCH AND CLINICAL PRACTICE 157 (2019) 107843.

2. Serrano, M.; Bouaid, A.; Martínez, M.; Aracil, J. Oxidation stability of biodiesel from di_erent feedstocks: Influence of commercial additives and purification step. Fuel **2013**, 113, 50–58.

3. (a) M. A. M. Gad-Elkareem, E. H. Abdelgadir, O. M. Badawy, A. Kadri, Potential antidiabetic effect of ethanolic and aqueous-ethanolic extracts of *Ricinus communis* leaves on streptozotocin-induced diabetes in rats, Peer Journal. (2019) DOI :10.7717/peerj.6441; (b) A. Aispuro-Pérez, J. López-Ávalos, F. García-Páez, J. Montes-Avila, L. A. Picos-Corrales, A. Ochoa-Terán, P. Bastidas, S. Montaño, L. Calderón-Zamora, U. Osuna-Martínez, J. I. Sarmiento-Sánchez, Synthesis and molecular docking studies of imines as α-glucosidase and α-amylase inhibitors, Bioorg. Chem. 94 (2020) 103491.

4. U. Etxeberria, A.L. de la Garza, J. Campion, J.A. Martínez , F.I. Milagro, Antidiabetic effects of natural plant extracts via inhibition of carbohydrate hydrolysis enzymes with emphasis on pancreatic alpha amylase, Expert Opin Ther Targets 16 (2012) 269–297.

5. H. Gao , B. Liu , P. Zhu , L.-J. Zhang , C.-P. Wan, G.-X. Rao , Z.-W. Mao, Synthesis and Biological Evaluation of New Piperazine Substituted 3, 5-Diarylisoxazolines, Current Organic Synthesis 16 (2019) 294-302.

6. M.A. Chiacchio , S.V. Giofrè , R. Romeo , G. Romeo , U. Chiacchio, Isoxazolidines as Biologically Active Compounds, Current Organic Synthesis 13 (2016) 726-749.

7. S. Ghannay, S. Bakari, A. Ghabi, A. Kadri, M. Msaddek, K. Aouadi, Stereoselective synthesis of enantiopure N-substituted pyrrolidin-2,5-dione derivatives by 1,3-dipolar cycloaddition and assessment of their in vitro antioxidant and antibacterial activities, Bioorg Med Chem Lett 27 (2017) 2302–2307.

8. S. Ghannay, S. Bakari, M. Msaddek, S. Vidal, A. Kadri, K. Aouadi, Design, synthesis, molecular properties and in vitro antioxidant and antibacterial potential of novel enantiopure isoxazolidine derivatives, Arab J Chem. 13 (2018) 2121-2131.

9. J. Brahmi, S. Ghannay, S. Bakari, A. Kadri, K. Aouadi, M. Msaddek, S. Vidal, Unprecedented stereoselective synthesis of 3-methylisoxazolidine-5-aryl-1,2,4-oxadiazoles via 1,3-dipolar cycloaddition and study of their in vitro antioxidant activity, Synth Commun. 46 (2016) 2037-2044.

10. S. L. Gaonkar, V.U. Nagaraj, S. Nayak, A Review on Current Synthetic Strategies of Oxazines, Mini-Reviews in Organic Chemistry 16 (2019) 43-58.

11. M. Berthet, T. Cheviet, G. Dujardin, I. Parrot, J. Martinez, Isoxazolidine: A privileged scaffold for organic and medicinal chemistry, Chem. Rev. 116 (2016) 15235-15283.

13. G. Periyasami, N. Arumugam, A. Aldalbahi, Inexpensive ionic liquid mediated green synthetic approach of multifunctionalized regioselective β-lactam fused isoxazolidine heterocyclic hybrids, Tetrahedron 73 (2016) 322-330.

13. (a) K. Aouadi, E. Jeanneau, M. Msaddek, J.-P. Praly, New synthetic routes toward enantiopure (2S,3R,4R)-4-hydroxyisoleucine by 1,3-dipolar cycloaddition of a chiral nitrone to C4 alkenes, Synthesis (2007) 3399–3405; (b) K. Aouadi, E. Jeanneau, M. Msaddek, J.-P. Praly, 1,3- Dipolar cycloaddition of a chiral nitrone to (E)-1,4-dichloro-2- butene: a new efficient synthesis of (2S,3S,4R)-4- hydroxyisoleucine, Tetrahedron Lett. 53 (2012) 2817–2821.

14. K. Aouadi, M. Msaddek, J.-P. Praly, Cycloaddition of a chiral nitrone to allylic motifs: an access to enantiopuresugar-based amino acids displaying a stable glycosidic bond and to 4(S)-4-hydroxy-L-ornithine, Tetrahedron 68 (2012) 1762–1768.

15. J. Brahmi, K. Aouadi, M. Msaddek, J.-P. Praly, S. Vidal, A stereoselective method for the synthesis of enantiopure 3-substituted 4-hydroxyproline derivatives via 1,3-dipolar cycloadditions, C. R. Chimie 19 (2016) 933-935.

16. K. Aouadi, J. Abdoul-Zabar, M. Msaddek, J.-P. Praly, Multi-Step Synthesis and Biological Evaluation of Analogues of Insulin Secretagogue (2S,3R,4S)-4-Hydroxyisoleucine, Eur. J. Org. Chem. (2009) 61-71.

17. S. Ghannay, F. Alminderej, M. Msaddek, J.-P. Praly, K. Aouadi, Design, synthesis, molecular properties and in vitro antioxidant and antibacterial potential of novel enantiopure isoxazolidine derivatives, ChemistrySelect 4 (2019) 5628-5632.

18. K. Aouadi, S. Vidal, M. Msaddek, J.-P. Praly, Cycloadditions of Chiral Nitrones to Racemic 3-Substituted Butenes: A Direct Access with Kinetic Resolution to Enantiopure Dihydroxylated Amino Acids, Synlett (2006) 3299–3303.

19. Crystal Data for compound **3g**. CCDC1975574, $C_{25}H_{36}N_2O_5$, M_r = 444.56, tetragonal, $P4_32_12$ (No. 96), a = 18.5811(6) Å, b = 18.5811(6) Å, c = 14.7124(6) Å, $\alpha = \beta = \gamma = 90^{\circ}$, V = 5079.6(4) Å^3, T = 150 K, Z = 8, Z' = 1, μ(MoK$_\alpha$) = 0.081, 33371 reflections measured, 6490 unique (R_{int} = 0.0694) which were used in all calculations. The final wR_2 was 0.2566 (all data) and R_1 was 0.0823 (I > 2(I)).

20. K. Aouadi, E. Jeanneau, M. Msaddek, J.-P. Praly, Analogues of insulin secretagogue (2S,3R,4S)-4-hydroxyisoleucine: synthesis by 1,3-dipolar cycloaddition reactions of chiral nitrones to alkenes, Tetrahedron Asymmetry 19 (2008) 1145–1152.

21. M. Qian, V. Nahoum, J. Bonicel, H. Bischoff, B. Henrissat, F. Payan, Enzyme-catalyzed condensation reaction in a mammalian alpha-amylase. High-resolution structural analysis of an enzymeinhibitor complex, Biochemistry 40 (2001) 7700–7709.

22. H. Mosbah, H. Chahdoura, A. Mannai, M. Snoussi, K. Aouadi, R. M. V. Abreu, A. Bouslama, L. Achour, B. Selmi, Biological Activities Evaluation of Enantiopure Isoxazolidine Derivatives: In Vitro, In Vivo and In Silico Studies, Applied Biochemistry and Biotechnology 187 (2019) 1113-1130.

23. L.K. Williams, C. Li, S.G. Withers, G.D. Brayer, Order and Disorder: differential structural impacts of myricetin and ethyl caffeate on human amylase, an antidiabetic target, J. Med. Chem. 55 (2012) 10177–10186.

24. E.H. Rydberg, C. Li, R. Maurus, C.M. Overall, G.D. Brayer, S.G. Withers, Mechanistic analyses of catalysis in human pancreatic α-amylase: Detailed kinetic and structural studies of mutants of three conserved carboxylic acids. Biochemistry 41 (2002) 4492–4502.

25. V. Roig-Zamboni, B. Cobucci-Ponzano, R. Iacono, M.C. Ferrara, S. Germany, Y. Bourne, G. Parenti, M. Moracci, G. Sulzenbacher, Structure of human lysosomal acid α-glucosidase–a guide for the treatment of Pompe disease. Nat. Commun. 8 (2017) 1111.

26. G. M. Morris, R. Huey, A. J. Olson, Using AutoDock for ligand-receptor docking, Current Protocols in Bioinformatics (2008) Chapter 8: Unit 8.14.

27. A. Pedretti, L. Villa, G. Vistoli, VEGA - an open platform to develop chemo-bio-informatics applications, using plug-in architecture and script programming. Journal of Computer-Aided Molecular Design 18 (2004) 167–173.

28. O. Trott, A. J. Olson, AutoDock Vina: Improving the speed and accuracy of docking with a new scoring function, efficient optimization, and multithreading, Journal of Computational Chemistry 31 (2010). 455–461.

29. E. F. Pettersen, T. D. Goddard, C. C. Huang, G. S. Couch, D. M. Greenblatt, E. C. Meng, T. E. Ferrin, UCSF Chimera--a visualization system for exploratory research and analysis, J Comput Chem. 25 (2004) 1605-1612.